

ON THE IMPORTANCE OF NEURAL WIENER FILTER FOR RESOURCE EFFICIENT MULTICHANNEL SPEECH ENHANCEMENT

Tsun-An Hsieh[†], Jacob Donley[‡], Daniel Wong[‡], Buye Xu[‡], Ashutosh Pandey[‡]

[†]Department of Intelligent Systems Engineering, Indiana University Bloomington, IN, USA

[‡]Reality Labs Research, Meta, WA, USA

ABSTRACT

We introduce a time-domain framework for efficient multichannel speech enhancement, emphasizing low latency and computational efficiency. This framework incorporates two compact deep neural networks (DNNs) surrounding a multichannel neural Wiener filter (NWF). The first DNN enhances the speech signal to estimate NWF coefficients, while the second DNN refines the output from the NWF. The NWF, while conceptually similar to the traditional frequency-domain Wiener filter, undergoes a training process optimized for low-latency speech enhancement, involving fine-tuning of both analysis and synthesis transforms. Our research results illustrate that the NWF output, having minimal nonlinear distortions, attains performance levels akin to those of the first DNN, deviating from conventional Wiener filter paradigms. Training all components jointly outperforms sequential training, despite its simplicity. Consequently, this framework achieves superior performance with fewer parameters and reduced computational demands, making it a compelling solution for resource-efficient multichannel speech enhancement.

Index Terms— Multichannel speech enhancement, low-compute and low-latency speech enhancement, neural beamforming

1. INTRODUCTION

Sequential neural beamforming has gained prominence as a potent technique for multichannel speech enhancement (SE), offering substantial improvements in performance [1, 2, 3, 4, 5, 6, 7, 8]. It generally contributes to an increased robustness of downstream applications, such as automatic speech recognition (ASR) [9, 10, 11, 8] and speaker verification [12, 13].

Sequential neural beamforming is characterized by a series of iterative steps. Initially, an enhancement network processes the multichannel audio input, extracting a less distorted speech signal. This processed signal serves as the target for estimating the spatial filter in the subsequent step, with the aim of further reducing nonlinear distortions. Subsequently, both the noisy mixture and the spatial filter estimate are passed to a second-stage enhancement network, culminating in the generation of the final enhanced speech. Optionally, the sequence of spatial filter estimation followed by enhancement network processing can be repeated multiple times to gradually improve the performance. Fig. 1 provides a visual overview of sequential neural beamforming.

Typically, sequential neural beamforming relies on underlying DNNs operating in the frequency-domain to enhance the short-time Fourier transform (STFT) of noisy speech [14, 4, 8, 15]. In addition, these systems often incorporate traditional spatial filters such as the multichannel Wiener filter (MCWF), minimum-variance distortionless response (MVDR) [16], and generalized eigenvalue (GEV) [17] beamformers. These traditional filters are valuable because they can

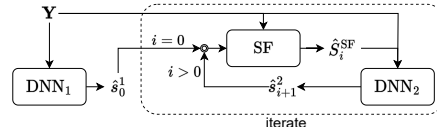


Fig. 1. A general workflow of sequential neural beamforming.

capture spectral patterns critical for isolating overlapping sources or dealing with reverberation. However, it is important to note that they have limitations, including numerical instability due to matrix inversion and the fact that filter coefficients are derived independently by solving a minimum mean squared error (MMSE) problem. As a result, jointly optimizing frequency-domain beamformers with deep neural networks (DNNs) can be challenging. To address the training instability associated with traditional spatial filters, a widely accepted strategy is to employ diagonal loading [18]. Furthermore, a recent study introduced the use of recurrent neural networks to directly estimate the matrix inverse, offering an alternative approach to mitigate training challenges [19].

In contrast, the advent of end-to-end systems has prompted some researchers to consider time-domain spatial filters as trainable components that can be jointly optimized with neural networks [1, 2, 3]. For instance, the filter-and-sum network (FaSNet) [2] employs a set of learnable filters that convolve with multichannel inputs, and their outputs are summed to produce the beamformed output. However, due to its end-to-end design, FaSNet may not guarantee certain desirable properties of traditional filters, such as a distortionless response or temporal consistency in filtering. A recent study by Luo et al. [3] addresses this limitation by introducing a time-domain generalized Wiener filter that derives filter coefficients using MMSE solution over a trainable latent representation.

While sequential neural beamforming has demonstrated effectiveness, the majority of research has been conducted in a non-causal setting, often neglecting resource constraints like computational demands, algorithmic latency, and model size [3, 8, 14]. While a few studies in the frequency domain, such as [4, 5, 15], have started considering these aspects, the exploration of end-to-end optimization in the time domain remains relatively unexplored. This is especially noteworthy, given the substantial potential of end-to-end optimization for resource-constrained speech enhancement [20, 21, 22].

We propose a novel time-domain sequential neural beamforming framework for resource efficient multichannel speech enhancement. This framework operates with an impressively low algorithmic latency of just 2 milliseconds, demonstrating remarkable efficiency in terms of both model parameters and computational demands. Central to our system are two lightweight, low-latency recurrent neural networks (LLRNNs) [21] employed as key DNN components, as de-

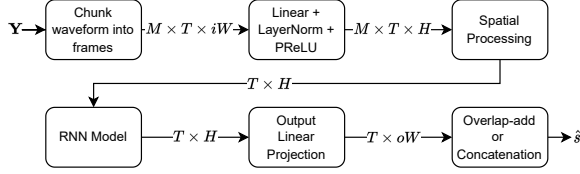


Fig. 2. Flow chart of LLRNN.

pictured in Fig. 1. These LLRNNs collaborate to simultaneously suppress noise and reverberation. Additionally, we introduce a novel neural Wiener filter (NWF) to function as the spatial filter, identified as the SF block in Fig. 1.

Given a multichannel noisy speech, the first-stage DNN (DNN₁) produces a single-channel enhanced speech that serves as the target signal for estimating NWF coefficients. The NWF conceptually resembles a traditional frequency-domain MCWF, with the key distinction being that its analysis and synthesis transforms are trained alongside other components. This adaptability allows these transforms to be fine-tuned for the specific requirements of low-latency speech enhancement, a task that may pose challenges for conventional filters. Subsequently, the multichannel noisy input is processed by the NWF, yielding a less distorted single-channel speech. The NWF output is then combined with the original input and fed to the second DNN (DNN₂) to obtain the final enhanced speech. Different blocks in the framework are setup in a way that stacking multiple blocks do not result in increased algorithmic latency.

To identify the optimal training approach, we conducted an extensive exploration of different training strategies, including various training orders for each module, combinations of pretrained weights, initialization methods, and loss configurations. We also provide extensive comparisons with competitive baseline models to showcase the promise of proposed framework for resource efficient speech enhancement.

2. PROPOSED METHOD

2.1. Problem Formulation

A multichannel signal recorded using an array with M microphones in a noisy and reverberant environment can be defined as $\mathbf{Y} = \{\mathbf{y}_m\}_{m=1}^M$, which includes M observations at M microphones. The m^{th} observation $\mathbf{y}_m \in \mathbb{R}^{1 \times L}$ with L samples can be decomposed as:

$$\mathbf{y}_m = \mathbf{s}_m^{\text{dir}} + \mathbf{s}_m^{\text{rev}} + \mathbf{z}_m^{\text{dir}} + \mathbf{z}_m^{\text{rev}} \quad (1)$$

where $\mathbf{s}_m^{\text{dir}}$, $\mathbf{s}_m^{\text{rev}}$, $\mathbf{z}_m^{\text{dir}}$, and $\mathbf{z}_m^{\text{rev}}$ respectively represent direct path speech, speech reverberation, direct path noise, and noise reverberation. The goal of multichannel speech enhancement system is get a close estimate of direct path speech $\mathbf{s}_r^{\text{dir}}$ at a given reference mic r .

2.2. Sequential Neural Beamforming

A general framework of sequential neural beamforming is shown in Fig. 1. Superscripts and subscripts respectively indicate the DNN and iteration index. Given a noisy mixture \mathbf{Y} , DNN₁ estimates an intermediate enhanced speech $\hat{\mathbf{s}}_0^1$. Next, a spatial filter uses $\hat{\mathbf{s}}_0^1$ as the target to obtain the beamformed speech $\hat{\mathbf{s}}_0^{\text{SF}}$, which is then concatenated with \mathbf{Y} across channel and processed by DNN₂ to obtain

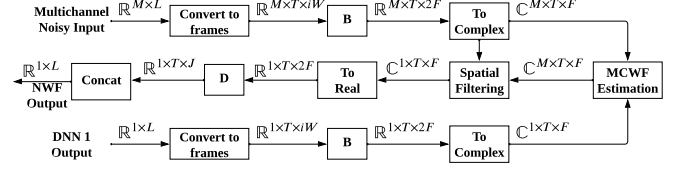


Fig. 3. Flow chart of the proposed NWF.

$\hat{\mathbf{s}}_1^2$. The output of the spatial filter contains minimal nonlinear distortions, and as a result, DNN₂ is expected to produce $\hat{\mathbf{s}}_1^2$ with improved nonlinear distortions. Optionally, the stack of spatial filter and DNN₂ can be repeated for $i \geq 1$ to obtain $\hat{\mathbf{s}}_i^{\text{SF}}$ and $\hat{\mathbf{s}}_{i+1}^2$.

2.3. Lightweight Low-latency RNN

The proposed framework incorporates two deep neural networks (DNNs), both of which are built upon a lightweight, low-latency Recurrent Neural Network (LLRNN) architecture introduced in [21]. Illustrated in Fig. 2, the LLRNN serves as a time-domain, multichannel speech enhancement model for processing noisy signal $\mathbf{Y} \in \mathbb{R}^{M \times L}$. The processing begins by converting \mathbf{Y} into a sequence of overlapping frames, employing a frame size of iW and a frame shift of J , resulting in $\bar{\mathbf{Y}} \in \mathbb{R}^{M \times T \times iW}$, where T signifies the number of frames. Prior to frame conversion, the signal is padded with $iW - J$ zeros at the beginning. Subsequently, a linear layer is applied, followed by layer normalization [23] and parametric rectified linear units (PReLU) [24], to project all frames into a latent representation of size H .

Following this, a spatial processing block is employed to reduce the channel dimension, mapping input of size $M \times T \times H$ to $T \times H$. The reduced feature tensors then traverse through B consecutive recurrent blocks, each comprising layer normalization followed by a Long Short-Term Memory (LSTM) [25] with a hidden size of H . Subsequently, all frames are linearly projected to the output frame size of oW using a linear layer, producing the sequence of enhanced frames.

The choice of the output frame size, whether it is oW or J (frame shift), depends on the specific stage of the LLRNN. If the LLRNN output serves as the final output for evaluation, the output frame size is set to oW , and overlap-add (OLA) is applied to obtain the enhanced signal. In this scenario, the LLRNN exhibits an algorithmic latency of oW , as oW samples in the output frame correspond to the rightmost oW samples in the input frame [21]. Alternatively, if the LLRNN output is fed into a subsequent model, the output frame size is set to J , and the enhanced signal is obtained by simply concatenating the output frames. This particular setup operates with an algorithmic latency of J . Importantly, in this setup, stacking multiple LLRNNs does not result in an increase in overall algorithmic latency due to the absence of OLA at intermediate stages.

2.4. Neural Wiener Filter

Fig. 3 shows the pipeline of our proposed NWF. The multichannel noisy input and the output from the first DNN are first converted to frames using a frame size of iW and frame shift of J . Both signals are padded with $iW - J$ zeros in the beginning before converting to frames. After this, they are projected to size $2F$ using analysis matrix \mathbf{B} and then converted to complex valued tensors by using the first half as the real part and the second half as the imaginary part.

Next, MCWF filter coefficients are estimated using the representation of the DNN_1 output as the target. A detailed description on how to estimate MCWF coefficients can be found in [4].

Next, spatial filtering is applied over the multichannel noisy transform to obtain a single-channel enhanced transform. The enhanced transform is converted to real-valued tensor by stacking real and imaginary parts side by side. Then, the synthesis matrix \mathbf{D} is multiplied with the real-valued enhanced transform to get enhanced frames of size J . Finally, all the enhanced frames are concatenated to obtain the enhanced signal. The algorithmic latency of this setup is J . If the NWF output is used as the final signal for evaluation, then the output frame size is set to oW and OLA is applied to obtain enhanced waveform with an algorithmic latency of oW .

It is important to note that the setup described here differs from the one in [3], where a real-valued Wiener filter was utilized. We observed that the real-valued formulation resulted in subpar performance compared to the complex-valued one. Similar to [4] and [26], the proposed NWF employs a frame-online approach utilizing Woodbury formula for matrix inversion during evaluation.

3. EXPERIMENTAL SETUP

3.1. Noisy Reverberant Data Simulation

To generate pairs of clean and noisy signals for training, we make use of the Interspeech 2020 DNS Challenge corpus [27]. The speakers in the training set are randomly divided into sets for training, testing, and validation, with a split ratio of 85%, 5%, and 10%, respectively. Similarly, the noises are categorized into distinct sets for training, testing, and validation. All the utterances are resampled to 16 kHz before being used for data generation.

Multichannel data is generated using an eight-microphone circular array with a radius of 10 cm. The data generation follows an algorithm outlined in previous studies [28, 29, 21]. We generate 80K training, 1.6K validation, and 3.2K test utterances.

We use Pyroomacoustics with an image method of order 6 to generate room impulse responses (RIRs). The dimensions of the rooms, including length, width, and height, are sampled uniformly from the ranges [3, 10] meters (m), [3, 10] m, and [2, 5] m, respectively. The absorption coefficients are sampled from [0.1, 0.4]. The number of noise sources is sampled from [1, 10]. The signal-to-noise ratio (SNR) is uniformly sampled from -10 to 10 dB, representing the ratio between the direct-path speech and interferences, excluding speech reverberation. The direct-path speech at the first microphone is used as the training target.

3.2. Model Configuration and Training

In this work, we consider six setups, including: (i) single-stage baselines, (ii) a DNN (DNN_1) followed by an NWF, (iii) DNN_1 followed by another DNN (DNN_2) without an NWF (iv) train DNN_1 and then jointly train a stack of DNN_1 , NWF and DNN_2 , (v) train a stack of DNN_1 and NWF together, and then jointly train a stack of DNN_1 , NWF and DNN_2 (vi) train a stack of DNN_1 , NWF and DNN_2 from scratch. These categories correspond to setups 1 to 6 in Table 1.

In particular, DNN_1 is an LLRNN model with a latency of 1 ms, employing parameters $H = 128$, $iW = 256$, and $oW = J = 16$. In (ii), we merge DNN_1 with NWF and utilize the NWF output, where a 2 ms latency is achieved by using $oW = 32$ with OLA in the synthesis transform. Case (iii) represents a simple dual-stage setup, where DNN_1 can be pretrained (or trained from scratch) and frozen

(or unfrozen) when training with DNN_2 . Similarly, (iv) through (vi) incorporate DNN_1 and DNN_2 around NWF. Here, DNN_1 and NWF use $oW = J = 16$ and concatenate output frames, while DNN_2 utilizes $oW = 32$ with OLA. The NWF maintains $F = 129$ across all cases.

In the aforementioned setups, multiple enhanced speech are generated, including those from DNN_1 , NWF, and DNN_2 . We conduct experiments to assess the effectiveness of minimizing loss at different outputs by simply adding different losses together.

We train various baseline models including LLRNN [21], MC-Conv-TasNet [20], MC-CRN [4], UXNet [22], and FSB-LSTM [15]. These models are tailored for single-stage processing, exhibiting latencies of either 2 ms or 4 ms. The LLRNN baseline achieves a latency latency of 2 ms by using $oW = 32$ (2 ms) with OLA.

For model optimization, we train these setups for 200 epochs using Adam optimizer [30] with a constant learning rate of 2×10^{-4} and *amsgrad* enabled. Following [21], we adopt the phase constrained magnitude (PCM) loss [31] to train all the models. In order to prevent unstable gradients, we clip gradient’s L^2 -norm to 0.03. Training for all setups is carried out on Nvidia V100 GPUs with automatic mixed precision.

3.3. Evaluation Metrics

Models are evaluated using perceptual evaluation of quality (PESQ), scale-invariant source-to-distortion ratio (SI-SDR), and short-time objective intelligibility (STOI) scores. Higher scores indicate better performance. The amount of computation is reported in Giga floating point operations (GFLOPs) for processing one second of 8-channel speech.

4. RESULTS

4.1. Baseline and Single-Stage Setups

Table 1 provides a comprehensive overview of performances and computational demands across all configurations. Scores from setup 0A pertain to the noisy reverberant mixture. An anticipated trend from 1A to 1F is evident, indicating improved performance with an increase in hidden size.

Setups 2A to 2F demonstrate the impact of combining DNN_1 with NWF. In 2A and 2B, NWF training is disabled, with signal transform initialized using DFT/iDFT coefficients, making them equivalent to traditional frequency-domain MCWF. Setups 2C to 2F employ NWF with trainable signal transforms. Notably, 2C and 2D initialize signal transforms with DFT coefficients, while 2E and 2F have randomly initialized transforms. Comparing to 1A and other configurations in Setup 2, setups with trainable NWFs exhibit improvements in STOI ranging from 4.44% to 6.48%. Across all experiments in Setup 2, optimal performance consistently occurs when calculating the loss using only NWF’s output.

Comparing 2C with 2E and 2D with 2F reveals a relatively minor impact of initialization. This implies a potential effective training strategy for DNN_1 +NWF is to randomly initialize NWF and jointly train DNN_1 and NWF using a loss at NWF output. Notably, NWF without trainable transforms (MCWF) performs significantly worse than 1A, underscoring the importance of optimizing analysis and synthesis transforms. Finally, objective scores from DNN_1 +NWF are similar to those of 1A, suggesting NWF’s potential to match a DNN performance while reducing nonlinear distortions.

Table 1. Model configurations and performance are summarized below. The symbols \checkmark and \times respectively denote the trainable and frozen modules. In the loss column, DNN_1 , NWF, and DNN_2 denote the outputs from these modules, utilized in calculating the loss. The total loss is derived by summing the losses from these modules.

Setup	STOI (%)	PESQ	SI-SDR (dB)	Update?	init _{NWF}	Loss	Latency (ms)	#params (M)	GFLOPs
0A Unprocessed	65.83	1.63	-7.48			N/A			N/A
1A LLRNN _{H=128}	80.8	2.27	2.9				2	0.44	1.34
1B LLRNN _{H=200}	83.9	2.43	4.2				2	1.03	2.78
1C LLRNN _{H=256}	85.6	2.51	4.9				2	1.66	4.25
1D LLRNN _{H=300}	86.2	2.56	5.3				2	2.26	5.61
1E LLRNN _{H=400}	87.5	2.64	6.0				2	3.97	9.40
1F LLRNN _{H=512}	88.3	2.69	6.5				2	6.46	14.79
1G MC-Conv-TasNet [20]	86.3	2.57	5.6	\checkmark	N/A	DNN_1	2	5.13	10.32
1H MC-CRN-2ms [4]	84.0	2.38	3.9				2	2.32	6.73
1I MC-CRN-4ms	85.7	2.51	4.7				4	2.32	6.73
1J UXNet-128 [22]	77.3	2.10	1.1				2	0.21	0.67
1K UXNet-256	80.9	2.25	2.9				2	0.81	2.12
1L FSB-LSTM [15]	88.2	2.68	5.8				4	1.97	7.80
2A	75.7	2.00	-1.3	\checkmark/\times	DFT	DNN_1			
2B	75.6	2.01	-0.3	\checkmark/\times	DFT	DNN_1 +NWF			
2C	82.0	2.14	3.2	\checkmark/\checkmark	DFT	NWF	1/2	0.51	2.82
2D	80.1	2.22	1.5	\checkmark/\checkmark	DFT	DNN_1 +NWF			
2E	82.0	2.18	3.4	\checkmark/\checkmark	Rand.	NWF			
2F	80.4	2.20	1.9	\checkmark/\checkmark	Rand.	DNN_1 +NWF			
3A DNN_1 + DNN_2	82.3	2.33	3.4	\checkmark/\checkmark		$DNN_1 + DNN_2$			
3B DNN_1 + DNN_2	82.9	2.36	3.8	\checkmark/\checkmark		DNN_2	1/2	0.87	2.74
3C DNN_1^{PT} + DNN_2	83.5	2.37	4.0	\checkmark/\checkmark	N/A	DNN_2			
3D DNN_1^{PT} + DNN_2	81.3	2.26	2.9	\times/\checkmark		DNN_2			
4A	82.6	2.36	3.0	$\times/\times/\checkmark$	DFT				
4B	82.3	2.31	3.0	$\checkmark/\times/\checkmark$	DFT				
4C	85.7	2.52	4.7	$\times/\checkmark/\checkmark$	Rand.	DNN_2	1/1/2	0.94	4.21
4D	86.4	2.52	5.6	$\checkmark/\checkmark/\checkmark$	Rand.				
5A	82.1	2.32	2.1	$\times/\times/\checkmark$	DFT				
5B	84.5	2.44	3.8	$\times/\times/\checkmark$	Rand.				
5C	84.5	2.43	3.7	$\times/\checkmark/\checkmark$	Rand.	DNN_2	1/1/2	0.94	4.21
5D	86.0	2.52	5.3	$\checkmark/\checkmark/\checkmark$	Rand.				
6A	84.9	2.46	4.0	$\checkmark/\checkmark/\checkmark$	Rand.	DNN_1 +NWF+ DNN_2			
6B	86.3	2.53	5.0	$\checkmark/\checkmark/\checkmark$	Rand.	NWF+ DNN_2	1/1/2	0.94	4.21
6C	87.4	2.58	6.0	$\checkmark/\checkmark/\checkmark$	Rand.	DNN_2			
6D $DNN_1^{200} + NWF + DNN_2^{200}$	89.1	2.70	7.0	$\checkmark/\checkmark/\checkmark$	Rand.	DNN_2	1/1/2	2.12	7.14

4.2. Dual-Stage Setups

In setup 3, we assess the performance of stacking two DNNs, DNN_1 and DNN_2 , without a NWF. We train all stages from scratch in 3A and 3B, while in 3C and 3D, we pretrain DNN_1 and subsequently train DNN_2 either independently or jointly with DNN_1 . These experiments indicate that the loss in the first stage is not beneficial, and pretraining DNN_1 is crucial for performance improvement. However, the results also reveal that incorporating multiple DNNs offers limited improvements.

Setups 4 and 5 explore various pretraining methods for stacking DNN_1 , NWF, and DNN_2 . In setup 4, 4A and 4B utilize MCWF, while 4C and 4D employ NWF. Results reveal superior performance of NWF over MCWF, with the optimal outcome observed when all components are jointly trained in 4D. Similarly, in setup 5, where DNN_1 is pretrained with Wiener filter, MCWF exhibits inferior performance compared to NWF. In 5B to 5D, we introduce random initialization of NWF in pretraining, followed by training NWF with DNN_2 and subsequently training DNN_1 and NWF with DNN_2 . While 5B and 5C yield comparable scores, 5D achieves the highest scores, aligning with the observed trend in setup 4.

In light of the insight that joint training leads to better performance, we conducted experiments in Setup 6, involving three distinct loss configurations and no pretraining. A noteworthy observation from 6A to 6C suggests that hitting the "sweet spot" for peak performance involves using the simplest setup—utilizing solely the

final output for loss and jointly training all components from scratch.

Our best system (6C) outperforms the baseline (1C) with comparable computational resources, demonstrating improvements in terms of STOI, PESQ, and SI-SDR by 1.82%, 0.07, and 1.14 dB, respectively, while employing only 56.63% of the parameters. Moreover, in comparison to 6C, model 1E requires 4.22 and 2.23 times more parameters and FLOPs to achieve a similar STOI score. Additionally, the best baseline model, FSB-LSTM, is surpassed by employing a larger LLRNN in both stages with a hidden size of 200. Remarkably, this improved performance is attained with reduced computational requirements, half the algorithmic latency, and a comparable number of parameters.

5. CONCLUSION

We have introduced a novel and resource-efficient framework for sequential neural beamforming in the time-domain, specifically designed for speech enhancement. Within this framework, we have incorporated a novel Neural Wiener Filter (NWF) to enhance low-latency speech processing. We have identified that the most effective training strategy involves simultaneous training of all components, with the final stage's output being used for loss computation. Our best-performing system outperformed robust baseline models across several key metrics, including speech quality, intelligibility, model size, and computational efficiency.

6. REFERENCES

- [1] K. Qian, Y. Zhang, S. Chang, X. Yang, D. Florencio, and M. Hasegawa-Johnson, "Deep learning based speech beamforming," in *ICASSP*, 2018.
- [2] Y. Luo, C. Han, N. Mesgarani, E. Ceolini, and S.-C. Liu, "FaS-Net: Low-latency adaptive beamforming for multi-microphone audio processing," in *ASRU*, 2019.
- [3] Y. Luo, "A time-domain real-valued generalized Wiener filter for multi-channel neural separation systems," *IEEE/ACM Transactions on Audio, Speech, and Language Processing*, vol. 30, pp. 3008–3019, 2022.
- [4] Z.-Q. Wang, G. Wichern, S. Watanabe, and J. Le Roux, "STFT-domain neural speech enhancement with very low algorithmic latency," *IEEE/ACM Transactions on Audio, Speech, and Language Processing*, vol. 31, pp. 397–410, 2022.
- [5] Y.-J. Lu, S. Cornell, X. Chang, W. Zhang, C. Li, Z. Ni, Z.-Q. Wang, and S. Watanabe, "Towards low-distortion multi-channel speech enhancement: The espnet-se submission to the l3das22 challenge," in *ICASSP*, 2022.
- [6] K. Kuang, F. Yang, J. Li, and J. Yang, "Three-stage hybrid neural beamformer for multi-channel speech enhancement," *The Journal of the Acoustical Society of America*, vol. 153, no. 6, pp. 3378–3378, 2023.
- [7] C.-H. Lee, C. Yang, Y. Shen, and H. Jin, "Improved mask-based neural beamforming for multichannel speech enhancement by snapshot matching masking," in *ICASSP*, 2023.
- [8] Z.-Q. Wang, S. Cornell, S. Choi, Y. Lee, B.-Y. Kim, and S. Watanabe, "TF-GridNet: Integrating full- and sub-band modeling for speech separation," *IEEE/ACM Transactions on Audio, Speech, and Language Processing*, vol. 31, pp. 3221–3236, 2023.
- [9] Z.-Q. Wang and D. Wang, "On spatial features for supervised speech separation and its application to beamforming and robust ASR," in *ICASSP*, 2018.
- [10] T. Ochiai, S. Watanabe, T. Hori, J. R. Hershey, and X. Xiao, "Unified architecture for multichannel end-to-end speech recognition with neural beamforming," *IEEE Journal of Selected Topics in Signal Processing*, vol. 11, no. 8, pp. 1274–1288, 2017.
- [11] W. Zhang, X. Chang, C. Boeddeker, T. Nakatani, S. Watanabe, and Y. Qian, "End-to-end dereverberation, beamforming, and speech recognition in a cocktail party," *IEEE/ACM Transactions on Audio, Speech, and Language Processing*, vol. 30, pp. 3173–3188, 2022.
- [12] L. Mošner, O. Plchot, L. Burget, and J. H. Černocký, "Multi-channel speaker verification with conv-tasnet based beamformer," in *ICASSP*, 2022, pp. 7982–7986.
- [13] S. Dowerah, R. Serizel, D. Jouvét, M. Mohammadamini, and D. Matrouf, "Compensating noise and reverberation in far-field multichannel speaker verification," 2022.
- [14] Zhong-Qiu Wang and DeLiang Wang, "Multi-microphone complex spectral mapping for speech dereverberation," in *ICASSP*, 2020, pp. 486–490.
- [15] Z.-Q. Wang, S. Cornell, S. Choi, Y. Lee, B.-Y. Kim, and S. Watanabe, "Neural speech enhancement with very low algorithmic latency and complexity via integrated full-and sub-band modeling," in *ICASSP*, 2023.
- [16] S. Doclo, S. Gannot, M. Moonen, and A. Spriet, "Acoustic beamforming for hearing aid applications," *Handbook on array processing and sensor networks*, pp. 269–302, 2010.
- [17] E. Warsitz and R. Haeb-Umbach, "Blind acoustic beamforming based on generalized eigenvalue decomposition," *IEEE Transactions on Audio, Speech, and Language Processing*, vol. 15, no. 5, pp. 1529–1539, 2007.
- [18] Xavier Mestre and Miguel A Lagunas, "On diagonal loading for minimum variance beamformers," in *International Symposium on Signal Processing and Information Technology*. IEEE, 2003, pp. 459–462.
- [19] Zhuohuang Zhang, Yong Xu, Meng Yu, Shi-Xiong Zhang, Lianwu Chen, and Dong Yu, "ADL-MVDR: All deep learning MVDR beamformer for target speech separation," in *ICASSP*, 2021.
- [20] J Zhang, C. Zorilă, R. Doddipatla, and J. Barker, "On end-to-end multi-channel time domain speech separation in reverberant environments," in *ICASSP*, 2020.
- [21] A. Pandey, K. Tan, and B. Xu, "A Simple RNN Model for Lightweight, Low-compute and Low-latency Multichannel Speech Enhancement in the Time Domain," in *INTER-SPEECH*, 2023.
- [22] K. Patel, A. Kovalyov, and I. Panahi, "UX-Net: Filter-and-process-based improved U-Net for real-time time-domain audio separation," in *ICASSP*, 2023.
- [23] J. L. Ba, J. R. Kiros, and G. E. Hinton, "Layer normalization," *arXiv preprint arXiv:1607.06450*, 2016.
- [24] K. He, X. Zhang, S. Ren, and J. Sun, "Delving deep into rectifiers: Surpassing human-level performance on imagenet classification," in *ICCV*, 2015.
- [25] S. Hochreiter and J. Schmidhuber, "Long short-term memory," *Neural Computation*, vol. 9, no. 8, pp. 1735–1780, 1997.
- [26] T. Higuchi, K. Kinoshita, N. Ito, S. Karita, and T. Nakatani, "Frame-by-frame closed-form update for mask-based adaptive MVDR beamforming," in *ICASSP*, 2018.
- [27] C. KA Reddy, V. Gopal, R. Cutler, E. Beyrami, R. Cheng, H. Dubey, S. Matuskevych, R. Aichner, A. Aazami, S. Braun, et al., "The INTERSPEECH 2020 deep noise suppression challenge: Datasets, subjective testing framework, and challenge results," *INTER-SPEECH*, 2020.
- [28] A. Pandey, B. Xu, A. Kumar, J. Donley, P. Calamia, and D. Wang, "Multichannel speech enhancement without beamforming," in *ICASSP*, 2022.
- [29] A. Pandey, B. Xu, A. Kumar, J. Donley, P. Calamia, and D. Wang, "TPARN: Triple-path attentive recurrent network for time-domain multichannel speech enhancement," in *ICASSP*, 2022.
- [30] D. P. Kingma and J. Ba, "Adam: A method for stochastic optimization," *arXiv preprint arXiv:1412.6980*, 2014.
- [31] A. Pandey and D. Wang, "Dense CNN with self-attention for time-domain speech enhancement," *IEEE/ACM Transactions on Audio, Speech, and Language Processing*, vol. 29, pp. 1270–1279, 2021.